Electronic Supplementary Material (ESI) for Sustainable Energy & Fuels.
This journal is © The Royal Society of Chemistry 2024

Supporting Information

Ammonia Storage Performance of Thiocyanate-Based Pseudo Ionic Liquids: Experimental Study and Computational Chemistry Analysis

Yu Cao, Kejie Jiang, Dongshun Deng*

Zhejiang Province Key Laboratory of Biofuel, College of Chemical Engineering, Zhejiang University of Technology, Hangzhou 310014, China.

***Corresponding author:**

Address: Zhejiang Province Key Laboratory of Biofuel, College of Chemical Engineering, Zhejiang University of Technology, Hangzhou 310014, China.

Email: dengdsh@zjut.edu.cn

Classical molecular dynamics (CMD) simulation details

The ratio of NH_3 to PILs in simulation box should correspond to actual NH_3 absorption capacity of each PIL, with the distribution of molecular quantities in each box as follows:

PILs	$[PIL]^+$	$[SCN]^-$	NH_3
[Im][SCN]	320	320	960
NH_4SCN	400	400	800
$[CH_3NH_3][SCN]$	400	400	800
$[CH_3CH_2NH_3][SCN]$	400	400	800
$[1,2,3\text{-TriZ}][SCN]_2$	280	560	840

Throughout all simulation processes, the same method was employed to handle non-bonded interactions: atom neighbor list was updated using the Verlet strategy to save computational time, long-range Coulomb interactions were calculated using the Particle Mesh Ewald (PME) method, and van der Waals forces were addressed with simple cutoff strategy. The cutoff distance for all three was set to 1.0 nm, consistent with original OPLS-AA force field documentation. Additionally, energy and pressure (EnerPres) corrections were used to account for long-range dispersion effects in systems.

Energy minimization was performed using conjugate gradient (cg) algorithm, with step size of 0.001 nm. Until system energy converged to 100 kJ/mol, the algorithm was terminated and structure with unreasonable contacts removed was output. Temperature and pressure control steps kept the internal temperature and pressure of the box at 298.15 K and 0.1 mPa, respectively, using the V-rescale temperature bath and the Berendsen pressure bath, lasting for 500 ps to allow system to equilibrate adequately. During equilibration simulation phase, pressure controlling method was switched to Parrinello-Rahman, continuing with NPT ensemble. The step size was set to 0.001 ps, with total simulation duration of 10 ns, outputting coordinates and energy information every 1000 steps. The 10,000 frames of atomic data produced during equilibrium simulation were used for subsequent analysis.

Ab initio molecular dynamics (AIMD) simulation details

A box with dimensions of 8×8×8 nm^3 was constructed using Packmol, containing 4 $[NH_4]^+$, 4 $[SCN]^-$, and 8 NH_3 molecules. Energy minimization was performed using GROMACS 2019.6 with OPLS-AA force field, setting Coulomb and van der Waals cutoff radii to 0.2 nm to eliminate unreasonable contacts within the box. The optimized structure from this process served as initial structure for AIMD calculations.AIMD simulations were performed with time step of 1.0 fs for a total of 10000 steps, with structure files output at each step. Three-dimensional periodic boundary conditions were applied to account for interactions between atoms in the box and surrounding. To save computational time, only γ point was considered during calculations. Atomic-centered basis set DZVP-MOLOPT-SR-GTH and plane-wave cutoff energy of 400 Ry were used to describe valence electrons, while GTH-BLYP pseudopotentials optimized for BLYP functional described core electrons. Density gradient approximation functional BLYP was used for electron distribution and system energy in self-consistent field (SCF) calculations. To improve efficiency, the convergence criterion for density matrix in SCF iterations was relaxed from 1×10^{-5} to 5×10^{-5}. Throughout the simulation, no SCF convergence failures occurred, and each frame of the structure files was carefully examined to ensure reasonable results.

Table S1 Detailed absorption data of PILs under ammonia at 0.1 MPa.

(a) for [Im][SCN]

Time (min)	Ammonia capacity (g NH_3/g PIL)			
	293.15 K	**303.15 K**	**313.15 K**	**323.15 K**
0	0	0	0	0
2	0.0509	0.05025	0.05352	0.04516
4	0.09714	0.0897	0.10264	0.09467
6	0.14774	0.13183	0.15456	0.14001
8	0.20211	0.17387	0.20094	0.18697
10	0.25397	0.22028	0.24527	0.22813
15	0.35953	0.30174	0.30255	0.26475
20	0.41922	0.34804	0.31213	0.27003
25	0.43561	0.36475	0.31291	0.27077
30	0.43931	0.36898	0.31352	0.27056
35	0.44051	0.3701	0.31355	0.27056
40	0.44268	0.37084	0.31345	
45	0.4423	0.37065		
50	0.44214	0.37078		

(b)for $[NH_4][SCN]$

Time (min)	Ammonia capacity (g NH_3/g PIL)			
	293.15 K	**303.15 K**	**313.15 K**	**323.15 K**
0	0	0	0	0
2	0.03943	0.0366	0.02436	0.02235
4	0.08795	0.07687	0.06263	0.06146
6	0.13571	0.11491	0.09921	0.0943
8	0.17929	0.14937	0.13085	0.12243
10	0.22646	0.19277	0.16409	0.15315
15	0.33762	0.27253	0.24683	0.21991
20	0.42662	0.33997	0.29577	0.24321
25	0.47447	0.37274	0.31326	0.24857
30	0.49265	0.38833	0.31896	0.25042
35	0.49977	0.39595	0.32045	0.25036
40	0.50216	0.39807	0.32179	0.25042
45	0.5033	0.39939	0.32189	0.25034
50	0.50378	0.40019	0.32184	
55	0.50429	0.40081	0.32173	
60	0.50433	0.40153		
70	0.50443	0.4017		
80	0.50437	0.4019		
90	0.50427	0.40205		
100		0.40197		

(c) for $[CH_3NH_3][SCN]$

Time (min)	Ammonia capacity (g NH_3/g PIL)			
	293.15 K	**303.15 K**	**313.15 K**	**323.15 K**
0	0	0	0	0
2	0.05055	0.04383	0.04554	0.04483
4	0.10999	0.09458	0.09086	0.09173
6	0.16976	0.15563	0.13546	0.13054
8	0.22224	0.2052	0.16785	0.15618
10	0.26595	0.24052	0.19349	0.16995
15	0.33155	0.27478	0.22015	0.17771
20	0.35071	0.27826	0.22283	0.17763
25	0.35621	0.27556	0.22251	0.17761
30	0.35607	0.27641	0.22251	
35	0.35436			

(d) for $[CH_3CH_2NH_3][SCN]$

Time (min)	Ammonia capacity (g NH_3/g PIL)			
	293.15 K	**303.15 K**	**313.15 K**	**323.15 K**
0	0	0	0	0
2	0.0329	0.04396	0.04572	0.03549
4	0.07053	0.08573	0.09347	0.07167
6	0.10739	0.13858	0.13555	0.10171
8	0.14531	0.16759	0.16325	0.12551
10	0.1797	0.19745	0.17738	0.13971
15	0.24351	0.22456	0.18313	0.14453
20	0.27904	0.23164	0.1828	0.14503
25	0.29039	0.23178	0.18208	0.14324
30	0.29046	0.23108		
35	0.29037			

(e) for [1,2,4-TriZ][SCN]$_2$

Time (min)	Ammonia capacity (g NH_3/g PIL)			
	293.15 K	**303.15 K**	**313.15 K**	**323.15 K**
0	0	0	0	0
2	0.01051	0.00719	7.73E-04	0.00948
4	0.02522	0.02419	0.0116	0.01227
6	0.03711	0.03772	0.02967	0.02799
8	0.04711	0.05836	0.0464	0.04327
10	0.06973	0.08161	0.06496	0.06863
15	0.118	0.13168	0.11192	0.11446
20	0.16989	0.17625	0.15276	0.14666
25	0.24281	0.21668	0.19058	0.17147
30	0.2918	0.2445	0.21933	0.18535
35	0.3113	0.26539	0.23754	0.18632
40	0.32478	0.28373	0.24007	0.18579
45	0.33515	0.29203	0.23972	
50	0.33754	0.29169	0.23951	
55	0.3371			

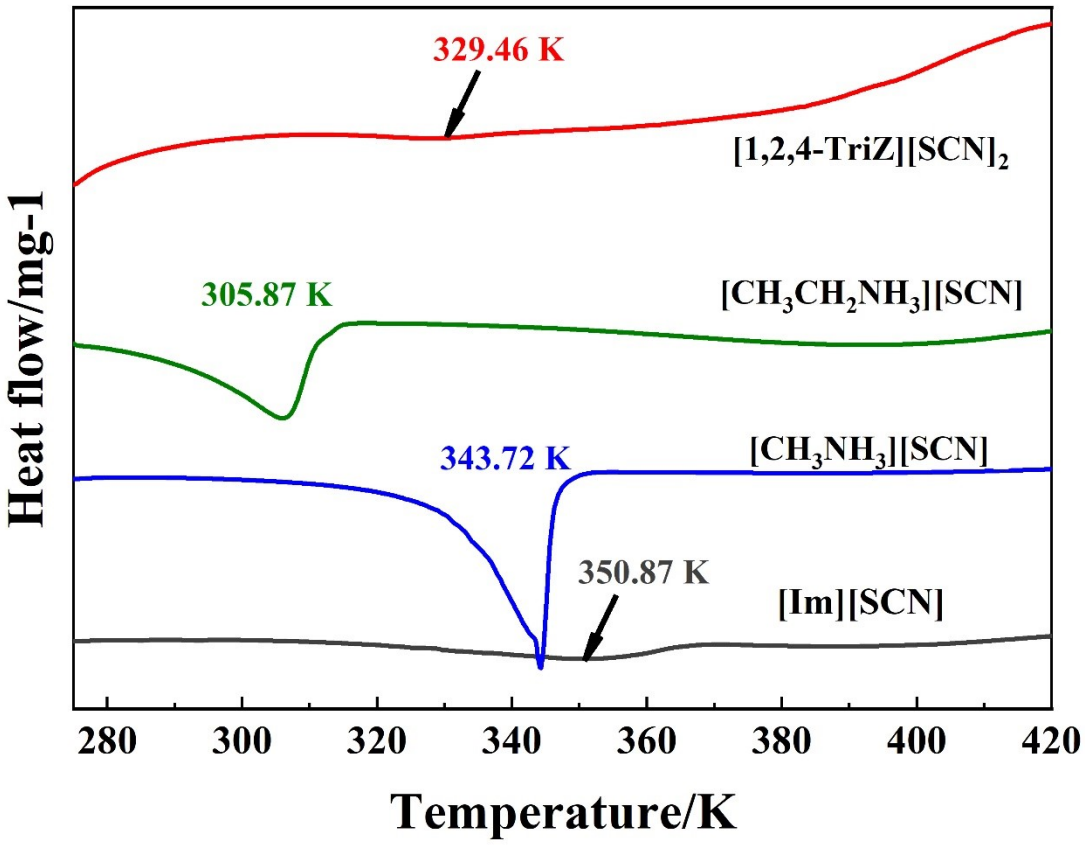

Fig. S1 Differential scanning calorimetry curves of PILs at 273 K-323 K.

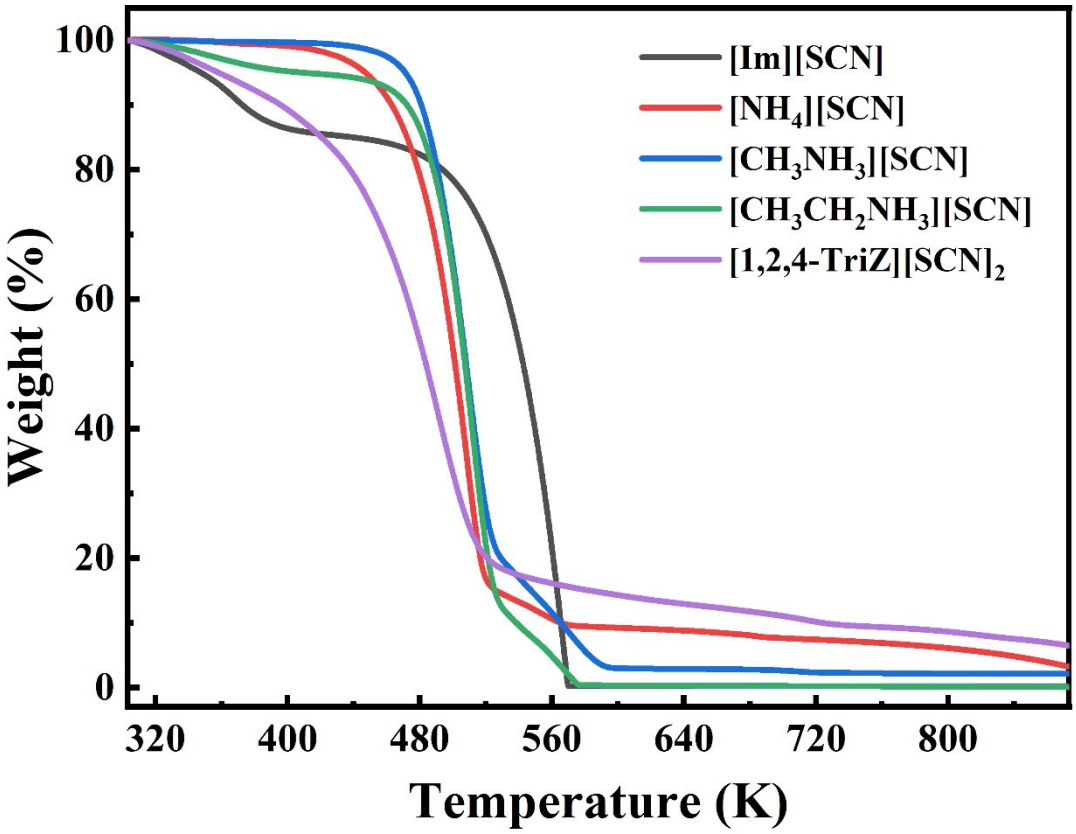

Fig. S2 Thermogravimetric analysis curves of PILs at 303.15 K-873.15 K.

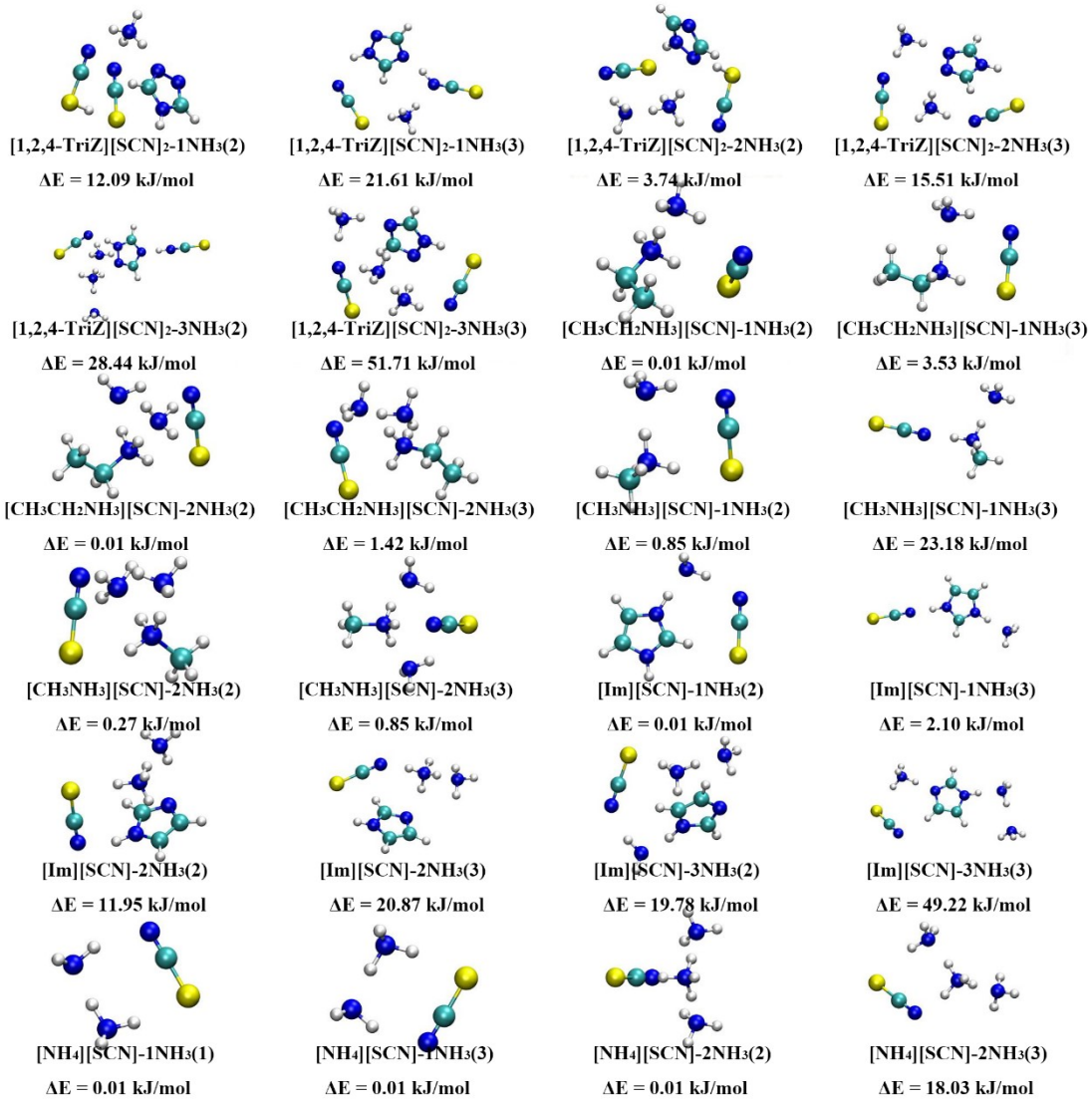

Fig. S3 Optimized structures with lower energy and energy difference with the most stable structure, blue, N; yellow, S; write, H and azure, C.

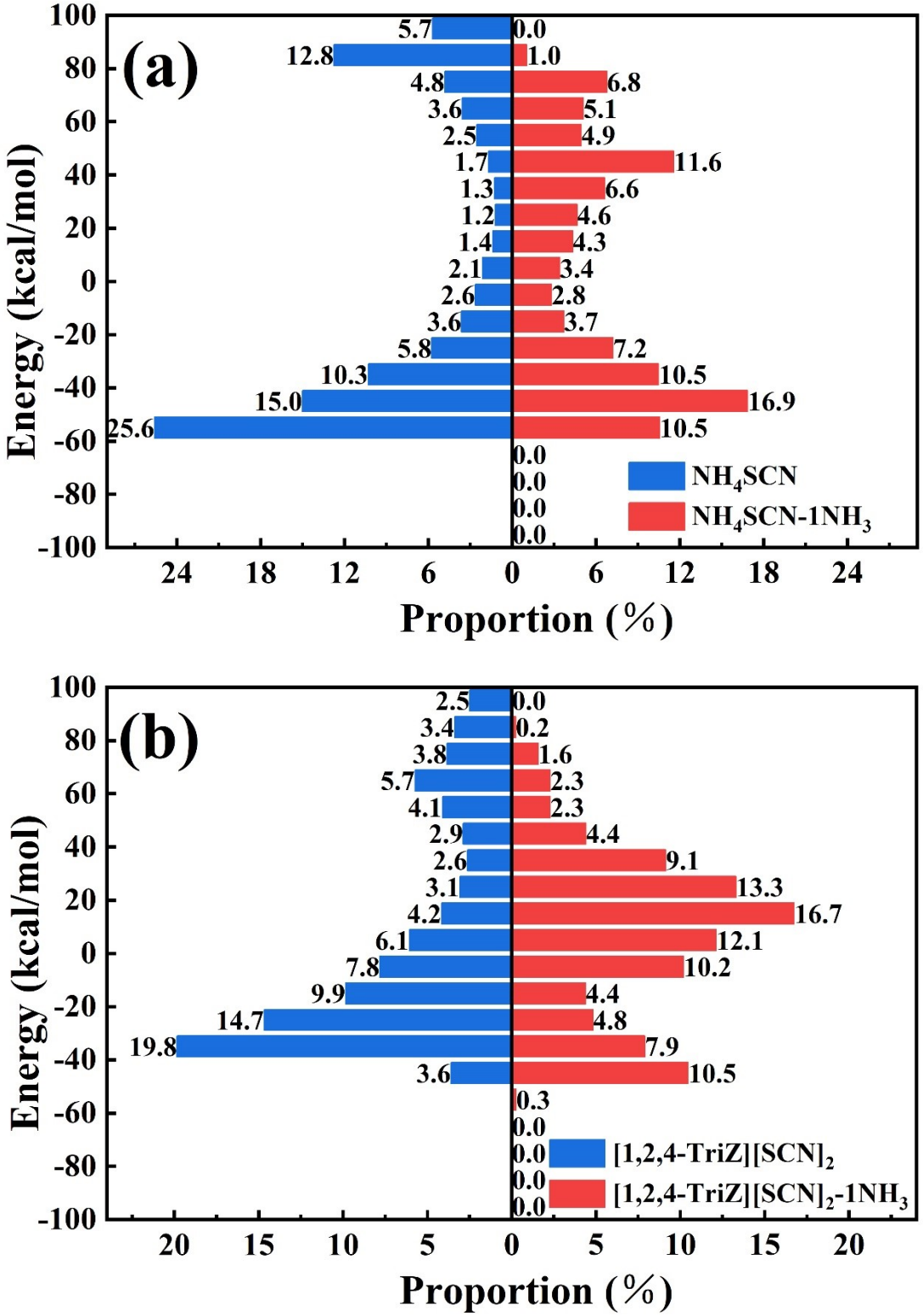

Fig. S4 Proportion of surface electrostatic potential distribution for (a) NH_4SCN and NH_4SCN-$1NH_3$; (b) [1,2,4-TriZ][$SCN]_2$ and [1,2,4-TriZ][$SCN]_2$-NH_3.

CMD Simulation of NH_4SCN in Vacuum-Sealed Box

The diffusion of NH_4SCN into NH_3 should be compared to the non-diffusion scenario of pure NH_4SCN. A rectangular box measuring 36×36×72 nm^3 was constructed, containing 800 NH_4SCN placed at the center along Z-axis ($18 < Z < 54$ nm), with vacuum layers at both ends. After energy minimization, this system was thermostatted to 298.15 K and subjected to 10 ns NVP simulation.

Fig. S5 shows the distribution of NH_4SCN at several time points, indicating observable deformations at the surfaces of NH_4SCN adjacent to vacuum layers as simulation progresses. However, the main body of the PIL layer remained complete. Even at 10 ns, no $[NH_4]^+$ or $[SCN]^-$ ions were observed to diffuse from the PIL layer into the vacuum regions. The solvent accessible surface area (SASA) of NH_4SCN within the box over time is shown in Fig. S6. Throughout 10 ns simulation, the SASA of NH_4SCN slightly decreased from 35 nm^2 to 34.5 nm^2, indicating no typical diffusion characteristic of surface fragmentation that would significantly increase the SASA. Both sets of data confirm that under the CMD simulation conditions, NH_4SCN does not spontaneously diffuse.

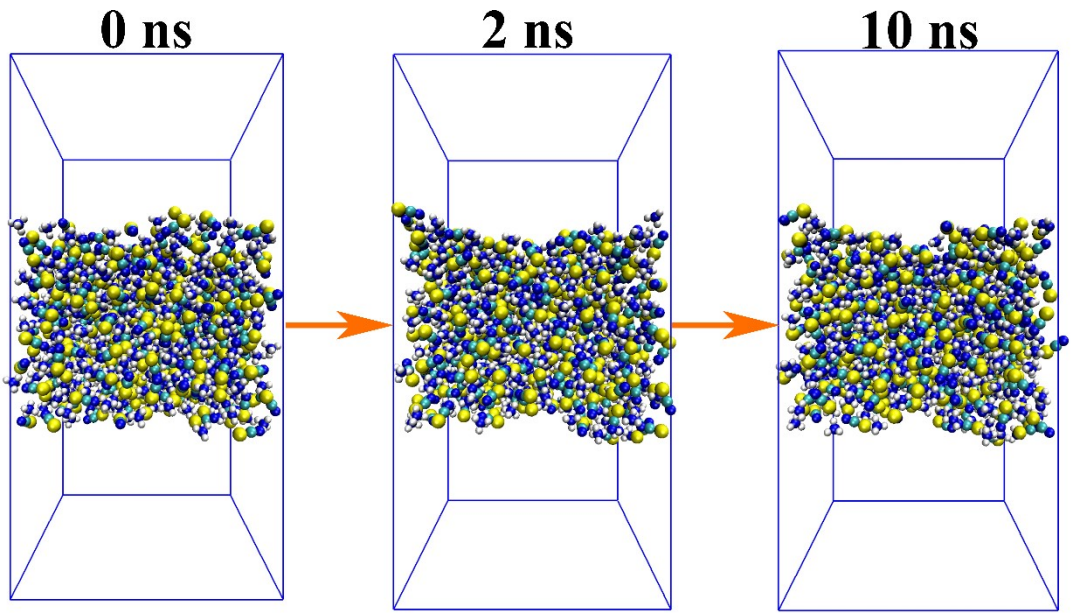

Fig. S5 Diffusion process of NH_4SCN in the vacuum-sealed box, blue, N; yellow, S; write, H and cyan, C.

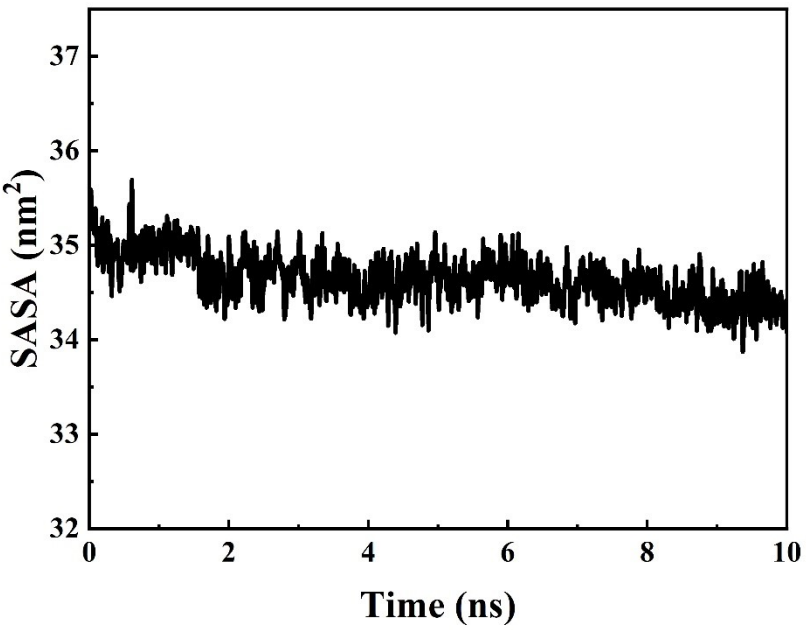

Fig. S6 Solvent Accessible Surface Area of NH4SCN Over Time